

METHODOLOGICAL NOTES

PACS numbers: **42.65.–k**, 42.65.Ky, 52.35.Mw

Bifurcation properties of the bremsstrahlung harmonics generated by a pumping field in plasmas

V P Silin, P V Silin

DOI: 10.1070/PU2007v050n07ABEH006311

Contents

1. **Introduction** **729**
2. **General starting relationships** **730**
3. **The pumping field** **730**
4. **The field of harmonics** **731**
5. **Efficiency of the generation of harmonics** **732**
6. **Bifurcation phenomenon in the degree of circular polarization of harmonics** **735**
7. **Conclusions** **738**
8. **Appendix** **739**

References **740**

Abstract. **Nonlinear generation of odd harmonics of the electromagnetic pumping field in a fully ionized plasma is briefly surveyed. Two threshold bifurcation properties of the harmonics are discussed, viz. the splitting of the peak of their intensity as a function of the degree of circular polarization of the pumping field and, at a somewhat higher threshold, the emergence of nonzero-intensity harmonics with complete circular polarization in a pumping field with a partial circular polarization.**

1. Introduction

The heating of electrons in a fully ionized plasma due to inverse bremsstrahlung absorption involves the energy transfer from ordered electromagnetic-field wave motion to the ordered motion of plasma electrons and the subsequent occurrence of random thermal motion of electrons due to chaotic electron – ion collisions, which is responsible for the electron heating. Such a plasma-heating process implies energy losses by the heating radiation in the plasma. Partially, this energy is emitted in the form of bremsstrahlung due to collisions between heated electrons and ions; in particular, under the action of the heating radiation, this results in a competition between the energy losses and the energy that can be released in the thermonuclear reactor [1].

Here, we concentrate on nonlinear optical phenomena that develop in a fully ionized plasma subjected to the electromagnetic radiation that oscillates at a frequency ω and gives rise to the ordered oscillatory motion of electrons. In reality, such motion proves to be nonlinear, e.g., in the sense that it nonlinearly depends on the strength of the electric field driving the electron motion and on the electromagnetic-field polarization [2]. The nonlinear motion of the electrons results, via electron – ion collisions, in the emission of a new (bremsstrahlung) electromagnetic field whose frequencies are multiples of the pumping-field frequency ω in plasma. We describe here the properties of the harmonics generated by the pumping field. In the Introduction, we will also touch upon some results that are not directly related to phenomena in fully ionized plasmas because the properties of these phenomena are not adequately interpreted.

The nonlinear optical phenomenon of the generation of higher electromagnetic-field harmonics in fully ionized plasmas was originally considered a fundamental phenomenon, irrespective of its possible applications. The more so as discussing practical applications at that time made publishing difficult and the applications themselves hardly realizable. However, the very possibility of substantial increases in the frequencies raised the problem of finding media with transparency bands for which high-frequency radiation sources might not correspond to then available sources. As a result, a quarter of a century after the publication of article [2], not only a theoretical but also an experimental science arose that was targeted at the problem of the generation of pumping-field harmonics, not only in plasmas but also in gases [3]. The field of research extended dramatically. To note several studies reflecting the scenario of such an evolution, let us mention Refs [3 – 12]. Among the reasons for such quick development was the passage to femtosecond pulses, which made it possible to increase the energy-flux density without constructing high-energy lasers. This led to a deeper insight into the properties of the generated harmonics, including the properties controlled by the generation process. In our view, some of these properties could be referred to as harmonic-generation-specified properties. One of these properties was

V P Silin, P V Silin P N Lebedev Physical Institute,
Russian Academy of Sciences,
Leninskii prosp. 53, 119991 Moscow, Russian Federation
Tel. (7-495) 132 63 24, (7-495) 132 68 71
E-mail: silin@sci.lebedev.ru, silinp@mail.ru

Received 11 December 2006, revised 7 January 2007
Uspekhi Fizicheskikh Nauk **177** (7) 763 – 775 (2007)
Translated by A V Getling; edited by A Radzig

experimentally revealed in Ref. [13] while studying the generation of the third harmonic of the pumping-laser field. The essence of the phenomenon is as follows. If a gas is directly exposed to intense radiation sufficient for ionization, the efficiency of generation proves to be very low; a subsequent laser pulse emitted after a virtually complete disappearance of ionization in the gas ensures, under otherwise identical conditions, an efficiency of generation of the third harmonic being almost two orders of magnitude higher than that of the first pulse. In the case of Ref. [13], this phenomenon was assigned to the fact that long-lived excited states are present in the gas plasma and, under certain conditions, they persist even after a virtually complete neutralization of the plasma. A theoretical model of hydrogenlike atom [14] demonstrated the extremely important role of such separately excited states, which substantially enhances the efficiency of generation of harmonics. In Ref. [15], the reasons for the l-degeneracy breaking were not discussed but rather an expressive example of manifestations of such a breaking was given.

Another effect [16] that has not yet been accounted for experimentally is the peak position of the harmonic-generation efficiency as a function of the degree of circular polarization of the pumping field at a certain finite value of the degree of circular polarization, rather than in the linear polarization limit. An explanation became possible after issuing Refs [11, 12]. However, more extensive experimental data are still needed to achieve adequate understanding of the phenomenon. By and large, it can be said that the harmonic-generation phenomenon calls for closer attention and more comprehensive fundamental research. Our review, which relies on a relatively simple model of the phenomenon, is aimed at interesting the reader in launching precisely such fundamental studies.

Below, we consider — and discuss from the standpoint of experimental research — the nonlinear bifurcation properties of the harmonics generated in plasmas.

In this context, the plasma constitutes the working body of a radiation oscillator in which the electromagnetic pumping field of frequency ω is transformed into the field of odd harmonics $(2n+1)\omega$, where n are positive integers. Such a situation is realized if the amplitude V_E of electron-velocity oscillations in the pumping field is small compared to the speed of light c:

$$V_E \equiv \frac{|e|E_1}{m\omega} \ll c\,, \tag{1}$$

where e is the elementary charge, m is the electron mass, and E_1 is the amplitude of the pumping-electric-field strength. In such a case of nonrelativistic motion of the electrons, the interaction between the pumping field and the electrons can be described in a dipole approximation. This corresponds to the possibility of neglecting both the spatial nonuniformity of the pumping field and the emerging magnetic field as factors affecting the electron motion.

2. General starting relationships

Since we restrict ourselves to a dipole approximation, the electrons can be described in terms of the kinetic equation of the form

$$\frac{\partial f}{\partial t} + \frac{e}{m}\,\mathbf{E}\,\frac{\partial f}{\partial \mathbf{V}} = J_{\mathrm{e}}[f]\,, \tag{2}$$

where f is the electron distribution function, $\mathbf{V}$ is the electron velocity, and $J_{\mathrm{e}} = J_{\mathrm{ee}} + J_{\mathrm{ei}}$ is the sum of the electron – electron and electron – ion collision integrals, J_{ee} and J_{ei}.

To describe the electric field, which we assume to be transversal ($\operatorname{div}\mathbf{E} = 0$), we use the equation

$$c^2\Delta\mathbf{E} - \frac{\partial^2\mathbf{E}}{\partial t^2} = 4\pi\,\frac{\partial\mathbf{j}}{\partial t}\,, \tag{3}$$

a consequence of the Maxwell equations, where the electric-current density is given by

$$\mathbf{j} = e\int \mathrm{d}\mathbf{V}\,\mathbf{V}f\,. \tag{4}$$

In our treatment, the polarization of radiation plays an important role. We will describe it following a classical book by Landau and Lifshitz [17]. Thus, the strength of the electric field at a given point in space is specified as

$$\mathbf{E}_0(t)\exp(-\mathrm{i}\omega t) + \mathbf{E}_0^*\exp(\mathrm{i}\omega t)\,.$$

The polarization properties of such a field are characterized by the polarization tensor

$$\rho_{\alpha\beta} = \frac{E_{0\alpha}E^*_{0\beta}}{\mathbf{E}_0\mathbf{E}_0^*} \qquad (\alpha, \beta = 1, 2 \to x, y)\,.$$

It can be written down as

$$\rho_{\alpha\beta} = \frac{1}{2}\begin{pmatrix} 1+\xi_3 & \xi_1 - \mathrm{i}\xi_2 \\ \xi_1 + \mathrm{i}\xi_2 & 1-\xi_3 \end{pmatrix},$$

where the parameters ξ_1, ξ_2, and ξ_3 (called the Stokes parameters) run from -1 to $+1$, $\xi_2 \equiv A$ is the degree of circular polarization of the field, and $(\xi_1^2 + \xi_2^2)^{1/2}$ is the degree of linear polarization.

In our consideration of the effect produced by the electromagnetic pumping field, we will use below the notation $A(1) \equiv A$ for its degree of circular polarization. We will denote the degrees of circular polarization of the harmonics as $A[2n+1, A, x]$, which corresponds to a nonlinear function of three arguments, viz. $2n+1$, the number of the harmonic; A, the degree of circular polarization of the pumping field, and $x = V_E/2V_T$, the dimensionless strength of the electric pumping field, where $V_T = \sqrt{k_{\mathrm{B}}T/m}$ is the thermal velocity of electrons with a temperature T.

3. The pumping field

We will assume that the electron collision rate is much smaller than the pumping-field frequency and will neglect the collisions in describing this field. Then, according to Eqn (2), the kinetic equation for the electron distribution function f_1 in the pumping field $\mathbf{E}_1$ assumes the simple (collisionless) form

$$\frac{\partial f_1}{\partial t} + \frac{e}{m}\,\mathbf{E}_1\,\frac{\partial f_1}{\partial \mathbf{V}} = 0\,. \tag{5}$$

A solution to this equation has the form

$$f_1(\mathbf{V}, t) = F\big(\mathbf{V} - \mathbf{u}(t)\big)\,, \tag{6}$$

where we use the Maxwellian distribution as the arbitrary function F:

$$F(\mathbf{V}) = \frac{N_e}{(2\pi)^{3/2} V_T^3} \exp\left(-\frac{mV^2}{2V_T^2}\right). \tag{7}$$

Here, N_e is the number density of electrons.

According to Eqns (4) and (6), one has

$$\mathbf{j}_1 = eN_e\,\mathbf{u}(t). \tag{8}$$

It follows from Eqn (5) that $\mathbf{u}(t)$ is the electron velocity in the pumping field; it is governed by the equation

$$\frac{\mathrm{d}\mathbf{u}}{\mathrm{d}t} = \frac{e\mathbf{E}_1}{m}. \tag{9}$$

Accordingly, Eqn (3) assumes the form

$$c^2\Delta\mathbf{E}_1 - \frac{\partial^2 \mathbf{E}_1}{\partial t^2} = \omega_{\mathrm{Le}}^2 \mathbf{E}_1, \tag{10}$$

where $\omega_{\mathrm{Le}} = \sqrt{4\pi e^2 N_e/m}$ is the electron Langmuir frequency.

Next, we use the solution to Eqn (10) in the form $\mathbf{E}_1(E_{1x}, E_{1y}, 0)$, with

$$\begin{aligned} E_{1x} &= e_x E\cos(\omega t - kz), \\ E_{1y} &= -e_y E\sin(\omega t - kz), \end{aligned} \tag{11}$$

where e_x and e_y are the polarization basis vectors ($e_x^2 + e_y^2 = 1$). Of particular interest to us is the degree of circular polarization of the pumping field, which has the following form in the case of Eqn (11):

$$A = -2e_x e_y. \tag{12}$$

Then, according to Eqn (9), one finds

$$\begin{aligned} u_x &= -e_x V_E \sin(\omega t - kz), \\ u_y &= -e_y V_E \cos(\omega t - kz). \end{aligned} \tag{13}$$

These expressions are the velocity-vector components of the nonrelativistic oscillatory motion of the electron in the pumping field (11) in the absence of electron–ion collisions.

4. The field of harmonics

In our presentation, we will utilize the same approach as in Refs [2, 11, 12, 18–20] and some results obtained therein. The efficiency of an approach for considering the generation of pumping harmonics via the bremsstrahlung mechanism was also demonstrated in Ref. [21] using a theoretical technique differing from ours.

In our treatment, the field of the generated harmonics is weak compared to the pumping field, as the corresponding perturbation of the electron distribution function is small compared to the distribution function relating to the pumping field. Therefore, the total electric field and the total distribution function can be written down as

$$\mathbf{E} = \mathbf{E}_1 + \delta\mathbf{E}, \qquad f = f_1 + \delta f. \tag{14}$$

Moreover, kinetic equation (2) can be linearized if f is replaced with f_1 in the collision integrals:

$$\frac{\partial \delta f}{\partial t} + \frac{e\mathbf{E}_1}{m}\frac{\partial \delta f}{\partial \mathbf{V}} + \frac{e\delta\mathbf{E}}{m}\frac{\partial f_1}{\partial \mathbf{V}} = J_{\mathrm{ee}}[f_1] + J_{\mathrm{ei}}[f_1]. \tag{15}$$

As can be seen from Eqn (3), there is no need to solve Eqn (15), and it is sufficient to multiply it by the electron charge and velocity and integrate with respect to velocity. Then, in view of the momentum conservation law for electron–electron collisions, which yields $\int \mathrm{d}\mathbf{V}\,\mathbf{V} J_{\mathrm{ee}}[f] = 0$, we obtain from Eqn (15):

$$\frac{\partial \delta\mathbf{j}}{\partial t} - \frac{e^2 N}{m}\,\delta\mathbf{E} = \frac{\partial \delta\mathbf{j}^{(r)}}{\partial t} \equiv \int \mathrm{d}\mathbf{V}\, e\mathbf{V} J_{\mathrm{ei}}[f_1]. \tag{16}$$

We took into account here that

$$\int \mathrm{d}\mathbf{V} f_1 = \int \mathrm{d}\mathbf{V} f = N_e, \qquad \delta\mathbf{j} = \int e\mathbf{V}\,\delta f\,\mathrm{d}\mathbf{V}. \tag{17}$$

Equation (16) makes it possible to write, according to Eqn (3), the following equation for the field of harmonics:

$$c^2\Delta\delta\mathbf{E} - \frac{\partial^2\delta\mathbf{E}}{\partial t^2} - \omega_{\mathrm{Le}}^2\,\delta\mathbf{E} = 4\pi\frac{\partial\delta\mathbf{j}^{(r)}}{\partial t} = 4\pi\int \mathrm{d}\mathbf{V}\, e\mathbf{V} J_{\mathrm{ei}}[f_1]. \tag{18}$$

This reduces the derivation of the equation for the field of harmonics to taking the integral on the right-hand side of Eqn (18), which represents the source of the fields of the harmonics generated due to electron–ion collisions.

To describe such collisions, we employ the Landau collision integral

$$J_{\mathrm{ei}}[F(\mathbf{V})] = \frac{2\pi e^2 e_i^2 N_i \Lambda}{m^2}\frac{\partial}{\partial V_j}\frac{V^2\delta_{jk} - V_j V_k}{V^3}\frac{\partial}{\partial V_k}F(\mathbf{V}), \tag{19}$$

where e_i is the ion charge, N_i is the number density of ions, and Λ is the Coulomb logarithm. We use Eqns (17), (6), and (7) to obtain

$$\frac{4\pi\,\partial\mathbf{j}^{(r)}}{\partial t} = -4\pi e N_e \frac{\sqrt{2}\,e^2 e_i^2 \Lambda N_i}{\sqrt{\pi}\,m^2 V_T^3}\int \mathrm{d}\mathbf{V}\,\frac{\mathbf{V}}{V^3}\exp\left(-\frac{(\mathbf{V}-\mathbf{u})^2}{2V_T^2}\right). \tag{20}$$

Since

$$\frac{\mathbf{V}}{V^3} = \mathrm{i}\int \frac{\mathrm{d}\mathbf{q}}{(2\pi)^3}\frac{4\pi}{q^2}\,\mathbf{q}\exp(-\mathrm{i}\mathbf{q}\mathbf{V}),$$

we can rewrite Eqn (20) in the form

$$\frac{4\pi\,\partial\mathbf{j}^{(r)}}{\partial t} = \mathrm{i}4\pi e N_e\frac{2e^2 e_i^2\Lambda N_i}{\pi m^2} \times \int \mathrm{d}\mathbf{q}\,\frac{\mathbf{q}}{q^2}\exp\left(-\mathrm{i}\mathbf{q}\mathbf{u}(t) - \frac{1}{2}q^2 V_T^2\right). \tag{21}$$

To represent the left-hand side of this formula as a harmonic expansion, we note that

$$-\mathbf{q}\mathbf{u}(t) = \frac{q}{2}V_E\sin\theta\big[(e_x+e_y)\sin(\omega t - \mathbf{k}\mathbf{r} + \varphi) + (e_x - e_y)\sin(\omega t - \mathbf{k}\mathbf{r} - \varphi)\big], \tag{22}$$

and, accordingly, one has

$$\exp[-\mathrm{i}\mathbf{q}\mathbf{u}(t)] = \sum_{l=-\infty}^{+\infty}\sum_{k=-\infty}^{+\infty} J_l\left(V_E q\sin\theta\,\frac{e_x+e_y}{2}\right) \times J_k\left(V_E q\sin\theta\,\frac{e_x-e_y}{2}\right) \times \exp[\mathrm{i}(l+k)(\omega t - \mathbf{k}\mathbf{r})]\exp[\mathrm{i}(l-k)\varphi]. \tag{23}$$

These relationships, together with Eqn (7), enable (see Appendix) writing the x projection of the right-hand side of Eqn (21) as

$$\frac{4\pi\,\partial j_x^{(r)}}{\partial t} = e_x E\omega_{\mathrm{Le}}^2\,\frac{\nu(E)}{\omega}\sum_{n=0}^{\infty}\sin\left[(2n+1)(\omega t - kz)\right] \times\left[A_n\left(\rho^2,\frac{V_E}{2V_T}\right) - A_{n+1}\left(\rho^2,\frac{V_E}{2V_T}\right)\right], \quad (24)$$

where $\rho^2 = e_x^2 - e_y^2 > 0$. Similarly, according to Eqns (21) and (A.8), we obtain

$$4\pi\,\frac{\partial j_y^{(r)}}{\partial t} = e_y E\omega_{\mathrm{Le}}^2\,\frac{\nu(E)}{\omega}\sum_{n=0}^{\infty}\cos\left[(2n+1)(\omega t - kz)\right] \times\left[A_n\left(\rho^2,\frac{V_E}{2V_T}\right) + A_{n+1}\left(\rho^2,\frac{V_E}{2V_T}\right)\right]. \quad (25)$$

Here, the following notation was used:

$$A_l(\rho^2, x) = \frac{2}{\sqrt{\pi}}\int_0^{x^2} \mathrm{d}t\,\sqrt{t}\,\exp(-t)\,I_l(\rho^2 t)\,, \quad (26)$$

and

$$\nu(E) = \frac{8\pi\sqrt{2}\,e^2 e_{\mathrm{i}}^2 \Lambda N_{\mathrm{i}}}{m^2 V_E^3} \quad (27)$$

is the rate of electron–ion collisions in a strong pumping field, for $V_E \gg V_T$, and $I_l(z)$ is the Bessel function of imaginary argument [22].

The field equation (18) and expressions (24) and (25) can be utilized to write down the field of harmonics as

$$\delta E_x = \sum_{n=0}^{\infty} E_x^{(2n+1)}\sin\left[(2n+1)(\omega t - kz)\right], \quad (28)$$

$$\delta E_y = \sum_{n=0}^{\infty} E_y^{(2n+1)}\cos\left[(2n+1)(\omega t - kz)\right], \quad (29)$$

where

$$E_x^{(2n+1)} = \frac{e_x E}{4n(n+1)}\,\frac{\nu(E)}{\omega}\left[A_n\left(\rho^2,\frac{V_E}{2V_T}\right) - A_{n+1}\left(\rho^2,\frac{V_E}{2V_T}\right)\right], \quad (30)$$

$$E_y^{(2n+1)} = \frac{e_y E}{4n(n+1)}\,\frac{\nu(E)}{\omega}\left[A_n\left(\rho^2,\frac{V_E}{2V_T}\right) + A_{n+1}\left(\rho^2,\frac{V_E}{2V_T}\right)\right]. \quad (31)$$

It is convenient in many cases to use the effective rate ν_{ei} of electron–ion collisions for a weak pumping field with $V_E \ll V_T$. Then, one finds

$$\nu_{\mathrm{ei}} = \frac{4\sqrt{2\pi}\,e^2 e_{\mathrm{i}}^2 \Lambda N_{\mathrm{i}}}{3m^2 V_T^3}\,. \quad (32)$$

Formulas (30) and (31) thus assume the form

$$E_x^{(2n+1)} = \frac{e_x E}{n(n+1)}\,\frac{3\sqrt{\pi}}{16}\,\frac{\nu_{\mathrm{ei}}}{\omega}\left[A_n(\rho^2, x) - A_{n+1}(\rho^2, x)\right]\frac{1}{x^3}\,, \quad (33)$$

$$E_y^{(2n+1)} = \frac{e_y E}{n(n+1)}\,\frac{3\sqrt{\pi}}{16}\,\frac{\nu_{\mathrm{ei}}}{\omega}\left[A_n(\rho^2, x) + A_{n+1}(\rho^2, x)\right]\frac{1}{x^3}\,. \quad (34)$$

The formulas obtained in this section will be employed below in considering the properties of the harmonics controlled by the circular polarization of the pumping field A, including bifurcation phenomena. Accordingly, we will use the relationship

$$A_n(\rho^2, x) \to A_n\left(\sqrt{1-A^2}\,,\, x\right). \quad (35)$$

5. Efficiency of the generation of harmonics

By the efficiency of the generation of harmonics we mean the time-averaged square of the harmonic-electric-field strength divided by the time-averaged square of the pumping-electric-field strength, namely

$$\eta_{\mathrm{eff}}^{(2n+1)} = \frac{\left\langle [\delta E_x^{(2n+1)}]^2 + [\delta E_y^{(2n+1)}]^2\right\rangle}{\left\langle [E_{1x}]^2 + [E_{1y}]^2\right\rangle}\,. \quad (36)$$

Here, the angle brackets denote averaging over the corresponding oscillation period. First of all, let us note that, according to Eqn (12), we have

$$\left\langle [E_{1x}]^2 + [E_{1y}]^2\right\rangle = \frac{1}{2}\,E^2\,. \quad (37)$$

Next, Eqns (28), (29), (33), and (34), with due account of Eqn (35), can be invoked to write down Eqn (36) in the following form

$$\eta_{\mathrm{eff}}^{(2n+1)} = D[2n+1, x, A]\left(\frac{\nu_{\mathrm{ei}}}{\omega}\right)^2, \quad (38)$$

where

$$D[2n+1, x, A] = \frac{9\pi}{256 n^2 (n+1)^2 x^6} \times\left[A_n^2\left(\sqrt{1-A^2}\,,\, x\right) + A_{n+1}^2\left(\sqrt{1-A^2}\,,\, x\right) - 2\sqrt{1-A^2}\,A_n\left(\sqrt{1-A^2}\,,\, x\right)A_{n+1}\left(\sqrt{1-A^2}\,,\, x\right)\right]. \quad (39)$$

We will analyze the phenomena described by formulas (38) and (39) using the diagrams for some harmonics with frequencies $(2n+1)\omega$.

For the third harmonic, Fig. 1 represents the surface corresponding to the function $D[3, x, A]$. It can be seen from this figure that the efficiency of generation of the third harmonic, which is determined by Eqn (39) as a function of the dimensionless pumping-electric-field strength x, first grows at relatively small x values and then, at larger values, decreases. Furthermore, as the degree A of circular polarization of the pumping field approaches the limits $A = +1$ and $A = -1$ of complete circular polarization, the generation efficiency for the third harmonic vanishes. However, the detailed pattern of the dependence of the function $D[3, x, A]$ on the degree of circular polarization of the pumping field proves to be relatively interesting, although it cannot be clearly seen from Fig. 1. To distinguish fine details, we first consider Fig. 2, which shows a portion of the same surface $D[3, x, A]$ representing the variations in the dimensionless pumping-electric-field strength at relatively large x, from 8 to 10. Here, the scale change compared to Fig. 1 reveals the trenching of this surface, which cannot be distinguished in Fig. 1.

It is natural to wonder at which x values such a trenching can emerge. An answer can be gotten from Fig. 3, where four

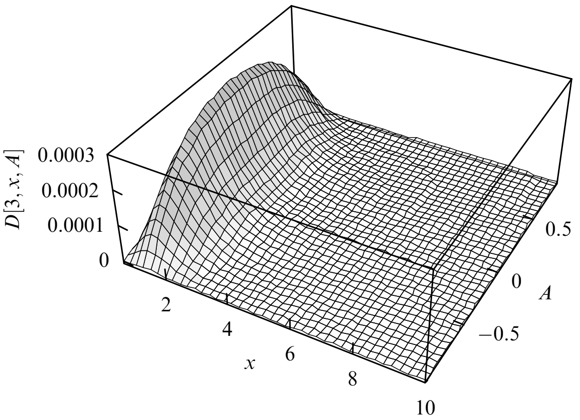

Figure 1. Surface representing the function $D[3, x, A]$, which characterizes the efficiency of generation of the third harmonic depending on the dimensionless pumping-electric-field strength $x = V_E/2V_T$ and the degree A of circular polarization of the pumping field.

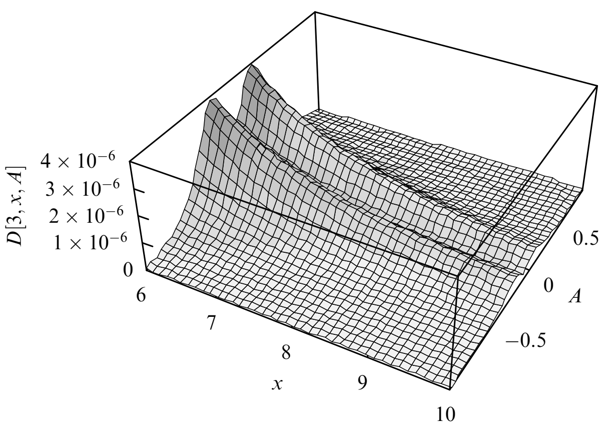

Figure 2. A portion of the $D[3, x, A]$ surface demonstrating the emergence of trenching.

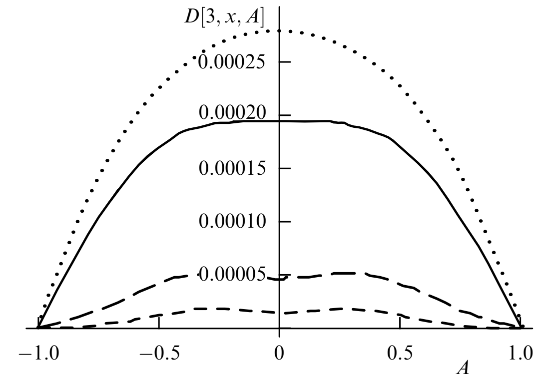

Figure 3. Four curves of a cross section of the $D[3, x, A]$-function surface at various values of the dimensionless pumping field: $x = 1$ (dotted curve), $x = 1.8042$ (solid curve), $x = 3$ (long-dashed curve), and $x = 4$ (short-dashed curve).

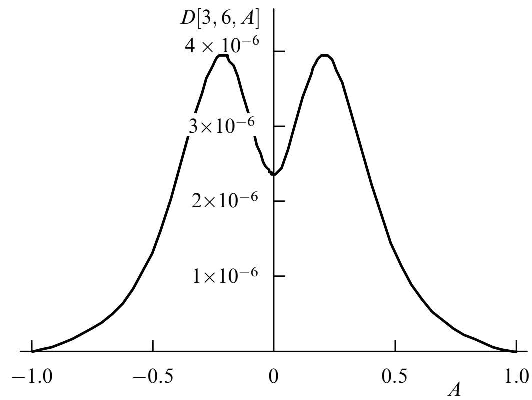

Figure 4. Cross-section curve of the surface of the function $D[3, x, A]$ at $x = 6$.

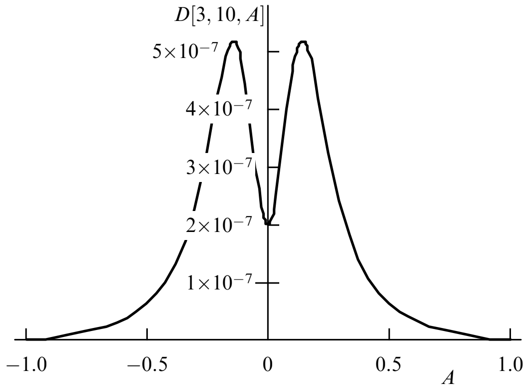

Figure 5. Cross-section curve of the surface of the function $D[3, x, A]$ at $x = 10$.

cross sections of the surface $D[3, x, A]$ are shown for $x = 1$ (dotted curve), $x = 1.8042$ (solid curve), $x = 3$ (long-dashed curve), and $x = 4$ (short-dashed curve). It is the solid curve that separates the region where $x^{\text{th.3}}_{\text{int.pol}} \cong 1.8042 > x$ and all curves of the cross section of the surface $D[3, A, x]$ are single-peaked from the region where $x^{\text{th.3}}_{\text{int.pol}} \cong 1.8042 < x$ and all curves of the cross section of the surface $D[3, A, x]$ are double-peaked. These peaks are weakly pronounced in Fig. 3 because of the relatively rapid drop of the function $D[3, x, A]$ with an increase in the dimensionless pumping-electric-field strength. To clearly distinguish the peak doubling in the curves of the cross section of the function $D[3, x, A]$, we present here Figs 4 and 5 for $x = 6$ and $x = 10$, respectively. It can be seen that the relative depth of the depression between the two peaks increases with x. We designate the emergence of two equal maxima of the function as the bifurcation phenomenon in the intensity of generation of the $(2n + 1)$th harmonic as a function of the degree of circular polarization of the pumping field. The corresponding dimensionless pumping-electric-field strength $x^{\text{th.}2n+1}_{\text{int.pol}}$, above which the doubling of maxima of the $D(2n + 1, x, A)$ function arises, will be referred to as the bifurcation threshold of the intensity of the $(2n + 1)$th harmonic.

The generality of the phenomenon under discussion can be recognized even in the case of the fifth harmonic. Our Figs 6 and 7 are qualitatively similar to Figs 1 and 2, thus reflecting the general trenching properties of the $D[5, x, A]$-function surface. The four cross sections of the $D[5, x, A]$ surface shown in Fig. 8 correspond to $x = 3.2$ (dotted curve), $x = 3.41257$ (solid curve), $x = 4.5$ (long-dashed curve), and $x = 6$ (short-dashed curve); they illustrate the division into

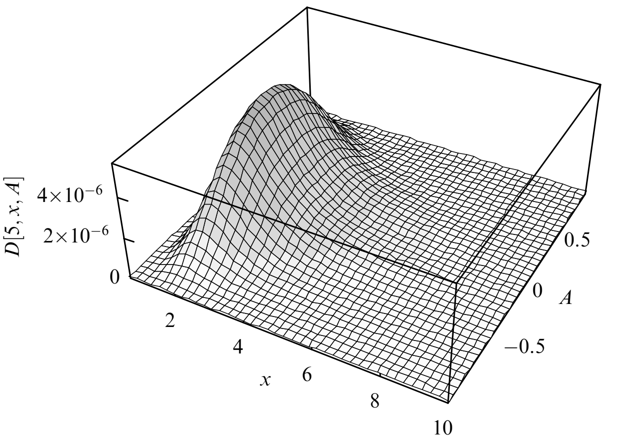

Figure 6. Surface of the function $D[5, x, A]$ characterizing the efficiency of generation of the fifth harmonic.

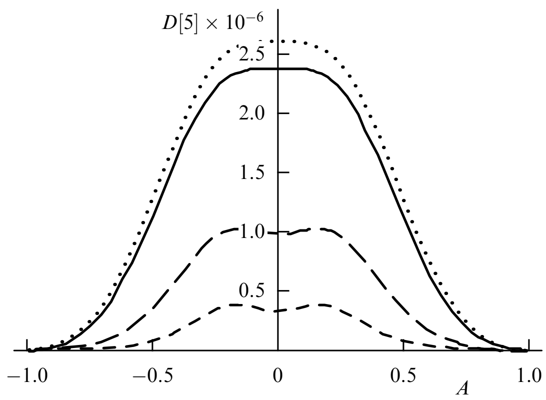

Figure 8. Four curves of a cross section of the $D[5, x, A]$-function surface at various values of the dimensionless pumping field: $x = 3.2$ (dotted curve), $x = 3.41257$ (solid curve), $x = 4.5$ (long-dashed curve), and $x = 6$ (short-dashed curve).

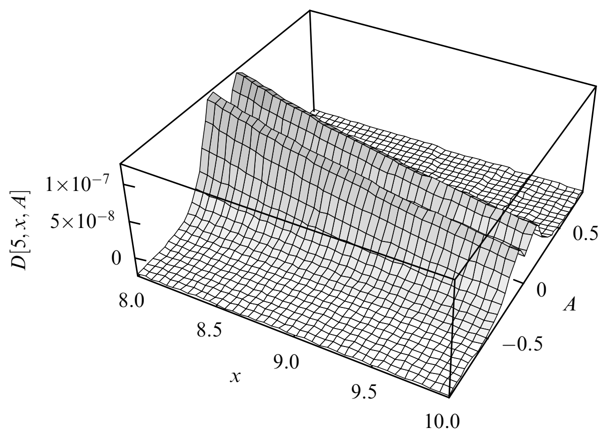

Figure 7. A portion of the surface of the $D[5, x, A]$ function demonstrating the emergence of trenching.

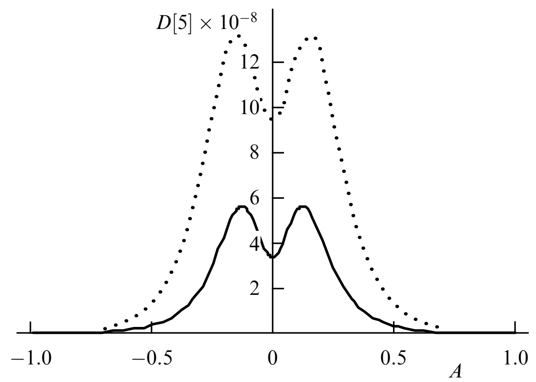

Figure 9. Two curves of a cross section of the $D[5, x, A]$-function surface clearly demonstrating the doubling of the generation-efficiency maxima for the fifth harmonic: dotted curve, $x = 8$; solid curve, $x = 10$.

the below-threshold ($x < x^{\mathrm{th}.5}_{\mathrm{int.\,pol}} = 3.41257$) and above-threshold ($x > x^{\mathrm{th}.5}_{\mathrm{int.\,pol}}$) regions. In the latter, the doubling of the $D[5, x, A]$-function peaks occurs. Since the peaks of the curves are not clearly distinguishable in Fig. 8, we also present here Fig. 9 which corresponds to the cross sections of the $D[5, x, A]$ surface at $x = 8$ (dotted curve) and $x = 10$ (solid curve). Here, the doubling of the cross-section peaks is obvious.

The peak-doubling phenomenon in the variation of the harmonic generation intensity at a given pumping-field strength can be clearly seen in the case of the seventh harmonic, which is demonstrated by Figs 10 and 11. However, we note first and foremost that, according to Fig. 10, the region of small values of the plotted function $D[7, x, A]$ at small x is now substantially broader compared to both the fifth (Fig. 6) and especially third (Fig. 1) harmonics. The formation of trenches at relatively large pumping-electric-field strengths ($8 < x < 10$) can be clearly recognized from Fig. 11. The trenching threshold, which corresponds to the doubling of the peaks of the cross-section curves of the $D[7, x, A]$ surface, can be seen from Fig. 12, where three such cross-section curves are depicted. The dotted curve corresponds to $x = 4$, the solid curve to the threshold of the bifurcation peak doubling at $x^{\mathrm{th}.7}_{\mathrm{int.\,pol}} = 4.8777$, and the short-dashed curve to the above-threshold value $x = 6$, at which two peaks can already be distinguished. Figure 13 shows double-peaked curves in the above-threshold region for $x = 6$ (short-dashed curve), $x = 7$ (heavy solid curve), and $x = 9$ (light solid curve).

The set of figures presented here for the third, fifth, and seventh harmonics can easily be extended to higher pumping-field harmonics. Their common property is the broadening of the region of small x values at which $D[2n+1, x, A]$ is especially small. As the number of the harmonic is increased further, the peak value of $D[2n+1, x, A]$ decreases. In particular, the following peaks were evaluated:

$$D(3)_{\max} \approx 3.2 \times 10^{-4}\,, \qquad D(5)_{\max} \approx 5.5 \times 10^{-6}\,,$$
$$D(7)_{\max} \approx 3.8 \times 10^{-7}\,, \qquad D(9)_{\max} \approx 5.8 \times 10^{-8}\,,$$
$$D(11)_{\max} \approx 4.3 \times 10^{-8}\,, \qquad D(13)_{\max} \approx 2.56 \times 10^{-9}\,.$$

These values are realized in the below-threshold region, for $x < x^{\mathrm{th}.2n+1}_{\mathrm{int.pol}}$. The above-presented analysis shows that the threshold field $x^{\mathrm{th}.2n+1}_{\mathrm{int.\,pol}}$ grows with the number of the harmonic. In particular, we obtained a threshold field of 1.8042 for the third harmonic, 3.4126 for the fifth, 4.8777 for the seventh, 6.325 for the ninth, 7.594 for the eleventh, and 9.1913 for the thirteenth. Thus, as the pumping-field strength increases, the maximum efficiency of generation of the given

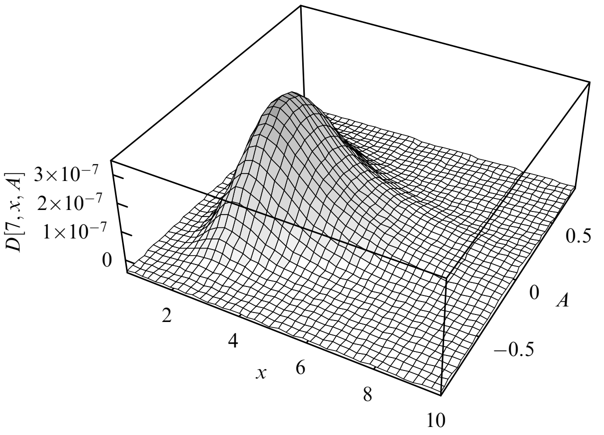

Figure 10. Surface of the function $D[7, x, A]$ characterizing the generation efficiency of the seventh harmonic.

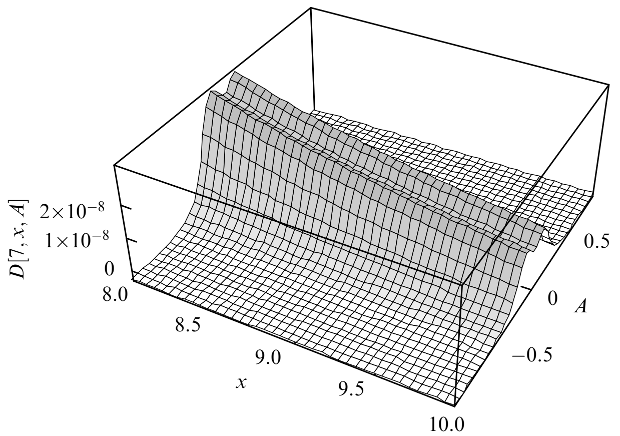

Figure 11. A portion of the surface of the $D[7, x, A]$ function for relatively high pumping-field strengths, which demonstrates the emergence of trenching.

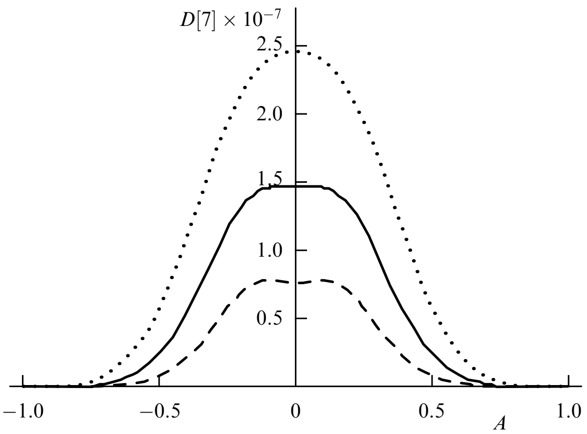

Figure 12. Three cross-section curves of the $D[7, x, A]$-function surface at various values of the dimensionless pumping field: $x = 4$ (dotted curve}, $x = 4.8777$ (solid curve), and $x = 6$ (short-dashed curve).

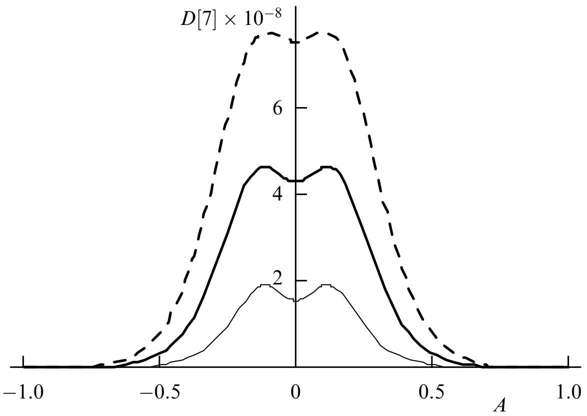

Figure 13. Three double-peaked cross-section curves of the $D[7, x, A]$-function surface for $x = 6$ (dashed curve), $x = 7$ (heavy solid curve), and $x = 9$ (light solid curve).

harmonic is first achieved at $A = 0$ and then, with a further growth of x and a decrease in the generation efficiency, the corresponding bifurcation value of the field is reached; as it is exceeded, two equal maxima of the generation efficiency of the harmonic develop at mutually opposite values of the degree of polarization of the pumping field. They are clearly pronounced if x substantially exceeds the bifurcation threshold of the generation efficiency of the harmonic. Naturally, if there are two maxima in the intensity of harmonic generation, the relative minimum corresponds to a zero value of the pumping-field polarization.

The influence of the circular polarization of the pumping field on the generation of harmonics in a gas was experimentally investigated in Ref. [16], and it could be believed that the gas was ionized at a certain stage of irradiation in these experiments. Whereas in previous studies of the same research group the efficiency of generation monotonically decreased with the growth of the degree of circular polarization of the pumping field, a substantially nonmonotonic behavior with a maximum at $A \neq 0$ was revealed in Ref. [16]. To account for this phenomenon, the mechanism whose theory was presented above had been invoked in Ref. [12].

We note finally that, in the framework of the model based on the Fock distribution function for electrons [23], the bifurcation-intensity threshold for the third harmonic was considered in Ref. [24] and, using a slightly different approach, in Ref. [12].

6. Bifurcation phenomenon in the degree of circular polarization of harmonics

To a certain extent, the phenomena discussed in this section were already revealed in Ref. [12], although they and, in particular, their threshold nature did not receive much attention there. A fairly detailed consideration and discussion of these phenomena were presented in Refs [25, 26], which were concerned with the polarization properties of the third harmonic; this harmonic is generated due to bremsstrahlung in a plasma produced by ionizing hydrogenlike atoms. The electron distribution function of such a fully ionized plasma was modelled by the distribution function of electrons resided on the nth energy level of the hydrogen atom, with the l-degeneracy of their states taken into account. Such a distribution function was obtained by Fock [23] and later on, independently, in Refs [27, 28]. The hypothesis for the universal nature of the bifurcation phenomenon discussed in Refs [25, 26] was put forward in the latter works and confirmed in Refs [18, 19], where a regular Maxwellian distribution was used instead of the Fock distribution. We will present below a theoretical view of the bifurcation phenomenon in the degree of circular polarization of harmonics using the results obtained earlier in Section 4.

The above-derived expressions (28)–(35), which describe the field of harmonics, make it possible to write down the polarization tensor of the field of harmonics in terms of the Stokes parameters (see above) and to obtain the following expression for $A[2n+1, x, A]$, the degree of circular polarization of the $(2n+1)$th harmonic:

$$\begin{aligned} A[2n+1, x, A] &= A\left[\left(A_n\left[\sqrt{1-A^2}, x\right]\right)^2 - \left(A_{n+1}\left[\sqrt{1-A^2}, x\right]\right)^2\right] \\ &\times \left[\left(A_n\left[\sqrt{1-A^2}, x\right]\right)^2 + \left(A_{n+1}\left[\sqrt{1-A^2}, x\right]\right)^2\right. \\ &\left. - 2\sqrt{1-A^2}\, A_n\left[\sqrt{1-A^2}, x\right] A_{n+1}\left[\sqrt{1-A^2}, x\right]\right]^{-1}. \end{aligned} \tag{40}$$

The diagrams presented below and based on this formula make it possible to understand the dependences of the degree of circular polarization on the pumping field, the strength of its electric field, and the degree of its circular polarization; in particular, the bifurcation phenomenon of the degree of circular polarization of harmonics will be demonstrated.

In this section, we start our consideration with the case of the third harmonic. First of all, let us obtain an expansion of function (40) at small x, the dimensionless strength of the pumping electric field. We restrict ourselves to the terms of order x^2, thus obtaining

$$A[3, x, A] \cong A\left\{1 + \frac{5}{14}(1 - A^2)x^2 + \ldots\right\}. \tag{41}$$

It can be seen from here that the complete circular polarization of the third harmonic, $|A(3)| = 1$, is possible only if the circular polarization of the pumping field is complete: $A^2 = 1$. However, as evident from the figures in the preceding section, harmonics are not generated in this limiting case. Moreover, we can state that $A = \pm 1$ are the limiting values of the pumping-field-polarization degree in the sense that the intensities of the third and other harmonics vanish in this limit. Due to the bremsstrahlung mechanism, this is a general property of the harmonic-generation process. However, the properties of harmonics become substantially richer at sufficiently strong pumping electric fields. This can be inferred from a careful observation of Fig. 14, which gives a three-dimensional representation of the surface of $A[3, x, A]$, the degree of circular polarization of the third harmonic as a function of the dimensionless pumping-electric-field strength x and the degree A of circular polarization of the pumping field. It may be seen (although with some difficulty) that the third harmonic proves to be completely polarized not only in the limits of $A = \pm 1$ but also at $|A|$ smaller than unity. To make this feature better distinguishable and to grasp the particularities of the behavior of the degree of circular polarization of the harmonic at sufficiently high degrees of circular polarization of the pumping field, we present here Fig. 15, in which four cross sections of the surface $A[3, x, A]$ are shown for $x = 1$ (dotted curve), $x = 2.02 \equiv x^{\text{th.3}}_{\text{bif. pol}}$ (solid curve corresponding to the bifurcation), $x = 5$ (long-dashed curve), and $x = 8$ (short-dashed curve).

We speak here of the circular-polarization bifurcation of the third harmonic and, in relation to the bifurcation curve, mean that $x^{\text{th.3}}_{\text{bif. pol}}$ is the circular-polarization-bifurcation threshold of the third harmonic. By such a bifurcation, we

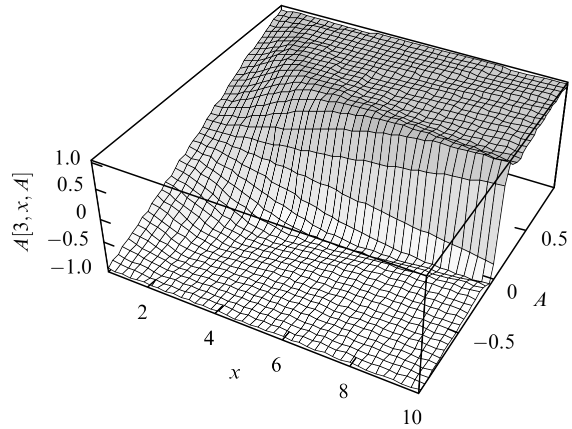

Figure 14. Surface corresponding to the function $A[3, x, A]$ that describes the degree of circular polarization of the third harmonic depending on the dimensionless strength x and the degree A of circular polarization of the pumping electric field.

understand a nonlinear phenomenon that manifests itself in a threshold manner as the pumping-electric-field strength is increased. Specifically, at small x, as follows from formula (41) and the dashed curve in Fig. 15, the degree of circular polarization of the third harmonic, $A[3, x, A]$, assumes unity magnitude and the circular polarization becomes complete only if the modulus of the degree of circular polarization of the pumping field, $|A|$, goes to unity. According to Figs 1 and 3, however, the intensity of the third harmonic vanishes in this limit. In other words, this property of $A[3, x, \pm 1]$ at x not exceeding the threshold value $x^{\text{th.3}}_{\text{bif. pol}}$ is a limiting property for the complete circular polarization of the third harmonic.

The situation changes in the above-threshold region, where $x > x^{\text{th.3}}_{\text{bif. pol}}$. As the dashed curves in Fig. 15 indicate, the complete circular polarization of the third harmonic corresponds not only to the limiting values for $|A| \to 1$ but also to a pair of values — a positive and a negative one — of the degree of circular polarization of the pumping field, which are smaller than unity in magnitude. Therefore, in the cross-section curves of the function $A[3, x, A]$, the doubling effect occurs in the values of the degree of circular polarization of the pumping field, at which the circular polarization of the harmonic is complete. This phenomenon, which we called the phenomenon of bifurcation doubling of the positions of complete circular polarization [25, 26], was discovered in plasmas with electron distributions differing from that assumed here. However, we already suggested then that this phenomenon is universal.

For plasmas with Maxwellian electron distributions, this suggestion was confirmed in Refs [18, 19] and partially considered in this section of our article for the third harmonic. We have shown [18] that the phenomenon of circular-polarization bifurcation also occurs for the fifth and seventh harmonics. Now, we will emphasize certain results of Ref. [18].

It should be noted here that Fig. 14 constructed for the third harmonic is also qualitatively correct for higher harmonics. We will not display here such graphs. Instead, let us consider analogs of Fig. 15. In particular, for the fifth harmonic, Fig. 16 shows four cross sections of the surface corresponding to the function $A[5, x, A]$, for four values of the dimensionless strength x of the pumping electric field. Specifically, the dotted curve corresponds to $x = 1$ and refers

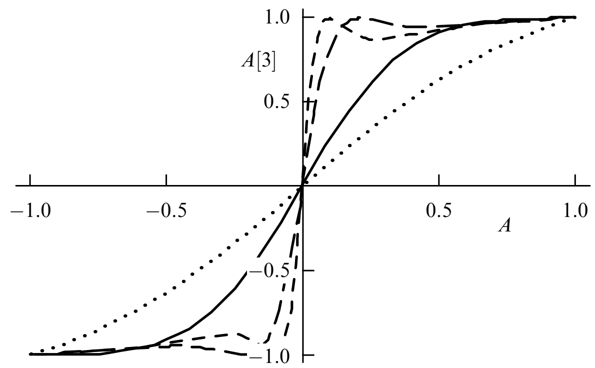

Figure 15. Four cross sections of the surface of the function $A[3, x, A]$ for several values of the dimensionless pumping-electric-field strength: dotted curve, $x = 1$; solid (bifurcation) curve, $x = 2.02$; long-dashed curve, $x = 5$ and short-dashed curve, $x = 8$.

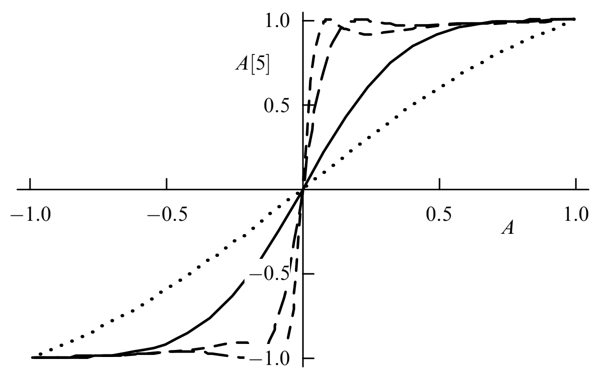

Figure 16. Four cross sections of the surface of the function $A[5, x, A]$ describing the degree of circular polarization of the fifth harmonic: dotted curve, $x = 1$; solid curve, $x = 2.39$ (the threshold field); long-dashed curve, $x = 6$, and short-dashed curve, $x = 10$.

to the below-threshold region; the solid curve to $x = 2.39 = x^{\text{th.5}}_{\text{bif. pol}}$, i.e., to the threshold field intensity that separates the below-threshold and above-threshold regions — this curve can thus be called the bifurcation curve; the long-dashed curve to $x = 6$, and the short-dashed curve to $x = 10$. The last two curves lie in the above-threshold region. They demonstrate the origin of the completely polarized fifth harmonic at relatively low magnitudes of the degree of circular polarization of the pumping field. For each above-threshold-cross-section curve there are two such degrees. This is a general property of the phenomenon of bifurcation doubling of the positions of complete circular polarization.

Even a comparison between Figs 15 and 16 leads us to the conclusion that both the third and fifth harmonics are almost completely — to a high accuracy — circularly polarized over a fairly wide range of variation in A, the degree of circular polarization of the pumping filed. This also applies to the seventh harmonic, as evident from Fig. 17 representing four cross-section curves of the surface corresponding to the function $A[7, x, A]$. Here, the dotted curve refers to $x = 1$, and the solid curve to $x = 2.7$, the bifurcation threshold of the degree of circular polarization of the seventh harmonic; the latter curve can thus be called the bifurcation curve. The two remaining curves (long-dashed curve for $x = 5$ and short-dashed curve for $x = 8$) relate to the above-threshold region. Both have a pair of points corresponding to complete circular

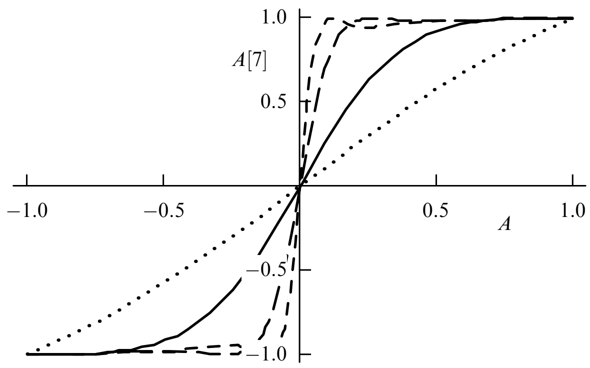

Figure 17. Four cross sections of the surface of the function $A[7, x, A]$ describing the degree of circular polarization of the seventh harmonic and demonstrating the bifurcation phenomenon in the degree of complete circular polarization with some related features: dotted curve, $x = 1$; solid curve, $x = 2.7$ (the bifurcation threshold of the degree of circular polarization of the seventh harmonic); long-dashed curve, $x = 5$, and short-dashed curve, $x = 8$.

polarization at small magnitudes of the degree of circular polarization. As in the cases of the third and fifth harmonics, the circular polarization of the seventh harmonic can be considered nearly complete ($A[7, x, A]$ is close to unity in magnitude) over a fairly wide range.

Lastly, Figs 15, 16, and 17 all indicate that the sign-reversal region of the degree of polarization of the almost completely circularly polarized harmonic shrinks with increasing x, the dimensionless pumping-field strength.

Since we are looking for a generality of the bifurcation phenomenon of the circular polarization of harmonics, let us dwell on the general equation describing the thresholds of this phenomenon for the $(2n + 1)$th harmonic. To this end, it is natural to apply the equation

$$\pm 1 = A\,\frac{\left(A_n\left(\sqrt{1 - A^2}, x\right)\right)^2 - \left(A_{n+1}\left(\sqrt{1 - A^2}, x\right)\right)^2}{B[2n + 1, x, A]}\,, \quad (42)$$

where the sign of the right-hand side coincides with that of the degree A of circular polarization of the pumping field, and

$$B[2n + 1, x, A] = \Big[A_n^2\left(\sqrt{1 - A^2}, x\right) + A_{n+1}^2\left(\sqrt{1 - A^2}, x\right) - 2\sqrt{1 - A^2}\, A_n\left(\sqrt{1 - A^2}, x\right) A_{n+1}\left(\sqrt{1 - A^2}, x\right)\Big]\,.$$

To find the threshold x value for the $(2n + 1)$th harmonic, we need to consider the consequences of Eqn (42) near $|A|^2 = 1$. To this end, we use the relationship

$$A_n\left(\sqrt{1 - A^2}, x\right) = \sum_{k=0}^{\infty} \frac{\left(\sqrt{1 - A^2}/2\right)^{n+2k}}{k!\,\Gamma(n + k + 1)}\,\gamma\left(n + \frac{3}{2} + 2k,\ x^2\right), \quad (43)$$

where $\Gamma(\alpha)$ is the Euler function, and $\gamma(\alpha, x)$ is the incomplete Euler function. With the aid of Eqn (43), we can write down a first approximation to Eqn (42) as

$$(1 - A^2)^{(n+1)}\left(\frac{\gamma(n + 3/2,\ x^2)}{\Gamma(n + 1)} - \frac{\gamma(n + 5/2,\ x^2)}{\Gamma(n + 2)}\right)^2 = 0\,. \quad (44)$$

The solution $A^2 = 1$ to this equation corresponds to zero values of the harmonics. Near the value of $A^2 = 1$ but for $A^2 \neq 0$, we obtain an equation for the bifurcation threshold

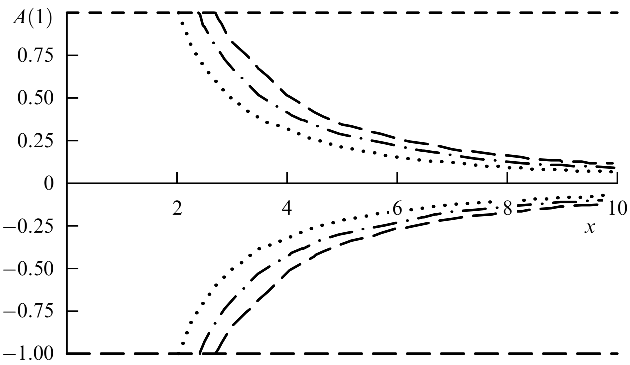

Figure 18. Loci of the complete circular polarization of the harmonics. The upper half of the diagram corresponds to $A[2n+1, x, A] = +1$, and the lower half to $A[2n+1, x, A] = -1$. The dashed horizontal straight lines $A(1) \equiv A = 1$ and $A(1) \equiv A = -1$ are the limiting sets for which the tendency to complete circular polarization is accompanied by the tendency to vanishing intensity of the harmonics. The points of the six curves relate to the x and A values at which the circular polarization of the harmonics is complete and their intensity differs from zero in the general case. The dotted curves correspond to the third harmonic, the dash-and-dot curves to the fifth harmonic, and the dashed curves to the seventh harmonic (cf. Ref. [7]).

of the complete circular polarization of the $(2n+1)$th harmonic. It has the form

$$\gamma\left(n+\frac{3}{2}\,,\,(x_{\text{bif. pol}}^{\text{th.}2n+1})^2\right) = \frac{1}{1+n}\,\gamma\left(n+\frac{5}{2}\,,\,(x_{\text{bif. pol}}^{\text{th.}2n+1})^2\right). \quad (45)$$

Numerical solutions of Eqn (45) for some harmonics are as follows:

$$x_{\text{bif. pol}}^{\text{th.(3)}} = 2.02\,, \quad x_{\text{bif. pol}}^{\text{th.(5)}} = 2.39\,, \quad x_{\text{bif. pol}}^{\text{th.(7)}} = 2.70\,,$$
$$x_{\text{bif. pol}}^{\text{th.(9)}} = 2.97\,, \quad x_{\text{bif. pol}}^{\text{th.(11)}} = 3.2\,, \quad x_{\text{bif. pol}}^{\text{th.(13)}} = 3.49\,,$$
$$x_{\text{bif. pol}}^{\text{th.(15)}} = 3.61\,, \quad x_{\text{bif. pol}}^{\text{th.(17)}} = 3.80\,, \quad x_{\text{bif. pol}}^{\text{th.(19)}} = 3.97\,,$$
$$x_{\text{bif. pol}}^{\text{th.(21)}} = 4.14\,, \quad x_{\text{bif. pol}}^{\text{th.(23)}} = 4.39\,, \quad x_{\text{bif. pol}}^{\text{th.(25)}} = 4.45\,,$$
$$x_{\text{bif. pol}}^{\text{th.(27)}} = 4.59\,, \quad x_{\text{bif. pol}}^{\text{th.(29)}} = 4.73\,, \quad x_{\text{bif. pol}}^{\text{th.(31)}} = 4.87\,,$$
$$x_{\text{bif. pol}}^{\text{th.(33)}} = 5.0\,.$$

It can be seen from these solutions that, up to fairly high harmonics, the threshold fields are located within a relatively narrow range of x values.

It should be noted that the existence of the general equation (45) and the solutions to it indicate that the phenomenon under discussion is universal in the framework of the adequacy of the theory applied.

Let us offer another illustration of the bifurcation phenomenon that follows from relationship (40) and solutions to Eqn (45). Specifically, we will present here the curves of the dependences that relate the degree A of circular polarization of the pumping field to the dimensionless strength x of the pumping electric field for the complete circular polarization of the third, fifth, and seventh harmonics. Figure 18 displays six curves; the upper three curves correspond to $A[2n+1, x, A] = 1$, and the lower three to $A[2n+1, x, A] = -1$. The dashed straight line at the top corresponds to the limiting value $A[2n+1, x, A] = 1$; in the bottom, to $A[2n+1, x, A] = -1$. The branching points in the dashed straight lines correspond to threshold x values. The dotted curves suit the third harmonic, the dash-and-dot curves the fifth harmonic, and the dashed curves the seventh harmonic. The branching of the curves of complete circular polarization, represented in Fig. 18, is among the simple properties of the bifurcation phenomenon discussed here.

7. Conclusions

The content of this article gives an idea of the properties of a nonlinear optical phenomenon, viz. the plasma bremsstrahlung due to a monochromatic pumping electromagnetic field. For nonrelativistic plasmas and nonrelativistic speeds of the electrons oscillating in the pumping field, the bremsstrahlung is represented by odd harmonics of the monochromatic pumping field. The theory of the considered bremsstrahlung, briefly presented above and in more detail in the Appendix, makes it possible to study the nonlinear properties of the harmonics depending on both the amplitude of the pumping-electric-field strength E and the degree of polarization of this field. We have demonstrated the following fact. Assume that the given pumping field is relatively weak and the intensity of the generated harmonics as a function of the degree of circular polarization of the pumping field reaches its maximum in the case of a linear polarization of this field ($A = 0$). In this case, if a certain threshold value $x_{\text{int. pol}}^{\text{th.}2n+1}$ of the pumping-field strength is exceeded, a pair of maxima arise at two values of the degree of circular polarization of the pumping field, equal in their magnitude and opposite in sign. We call this phenomenon the intensity bifurcation of the bremsstrahlung in the pumping-field harmonics; it manifests itself in a doubling of the intensity maxima of the harmonics.

As the pumping intensity increases, another bifurcation property of harmonics becomes notable. At relatively low pumping intensities, the complete circular polarization of the harmonics corresponds to their zero intensity. In other words, if the polarization of the harmonics tends to become circular at such intensities, their intensity vanishes. This property is also present at high pumping-field intensities and is described by the straight lines $A = 1$ and $A = -1$ (Fig. 18). However, as the dimensionless pumping-field strength reaches its threshold value $x_{\text{int. pol}}^{\text{th.}2n+1}$ for the given harmonic, curves branch off such straight lines; these curves correspond to the complete circular polarization of the $(2n+1)$th harmonic and to the degrees of circular polarization at which the intensity of the harmonics differs from zero.

In addition to such a bifurcation of the degrees of polarization of the pumping field that lead to the complete circular polarization of the harmonics, the following fact should be noted. For the generated harmonics, fairly wide ranges of the degrees of circular polarization of the pumping field (close to either $A = +1$ or $A = -1$) emerge, in which the complete polarization of the harmonics is, to a high accuracy, virtually circular. At the same time, the region of the transition from negative to positive degrees of circular polarization of the harmonics shrinks with the increase in the dimensionless pumping-field strength. These properties appear to accompany the bifurcation phenomenon of the complete circular polarization of the harmonics.

Let us present here a formula that expresses the pumping energy flux density q in terms of the parameter x:

$$q \cong x^2 \left(\frac{k_{\text{B}} T\,[\text{eV}]}{25}\right) \left(\hbar\omega\,[\text{eV}]\right)^2 \times 1.7 \times 10^{14}\ \text{W cm}^{-2}\,, \quad (46)$$

where the temperature is measured in units of 25 eV, and the pumping-field frequency in electron-volts. If the threshold of the position bifurcation in the third-harmonic intensity is $x = 1.8042$, formula (46) yields

$$q^{\text{th}(3)}_{\text{int. pol}} \equiv \left(\frac{k_{\text{B}} T\,[\text{eV}]}{25}\right) \big(\hbar\omega\,[\text{eV}]\big)^2 \times 5.5 \times 10^{14}\ \text{W cm}^{-2}\,.$$

Accordingly, for the bifurcation threshold of the degree of circular polarization of the third harmonic, with $x = 2.02$, we obtain

$$q^{\text{th}(3)}_{\text{bif. pol}} \cong \left(\frac{k_{\text{B}} T\,[\text{eV}]}{25}\right) \big(\hbar\omega\,[\text{eV}]\big)^2 \times 6.9 \times 10^{14}\ \text{W cm}^{-2}\,.$$

The excess of the second threshold over the first one is a general property of the harmonics generated in fully ionized plasmas due to collisions between the electrons oscillating in the pumping field and ions.

We note that the steadfast interest in the generation of harmonics partially stems from the fact that progress on the problem of harmonic generation leads to the possibilities of creating short pulses; they, as is known, result in high radiation energy flux densities at relatively low energies of the laser pulse after its shortening.

Acknowledgments
This work was supported in part by the Ministry of Education and Science of the Russian Federation (state contract No. 02-445-11-7331), INTAS (grant No. 05-51-5037), and the Russian Foundation for Basic Research (project No. 05-02-16897).

8. Appendix

We use the relationship

$$\exp(\mathrm{i}z\sin\varphi) = \sum_{k=-\infty}^{+\infty} J_k(z)\exp(\mathrm{i}k\varphi)$$

to take the integral

$$\begin{aligned}
I_x &= \int \mathrm{d}\mathbf{q}\,\frac{q_x}{q^2}\exp\left(-\mathrm{i}\mathbf{qu} - \frac{1}{2}\,q^2 V_T^2\right) \\
&= \int_0^\infty \mathrm{d}q\,q\exp\left(-\frac{1}{2}\,q^2 V_T^2\right)\int_0^\pi \sin^2\theta\,\mathrm{d}\theta \int_0^{2\pi}\mathrm{d}\varphi\cos\varphi \\
&\times \sum_{l=-\infty}^{+\infty}\sum_{n=-\infty}^{+\infty} J_l(qV_E\,\alpha\sin\theta)\,J_n(qV_E\,\beta\sin\theta) \\
&\times \exp\big[\mathrm{i}(l+n)(\omega t - kz)\big]\exp\big[\mathrm{i}(l-n)\varphi\big] \\
&= \pi\int_0^\infty \mathrm{d}q\,q\exp\left(-\frac{1}{2}\,q^2 V_T^2\right)\int_0^\pi \sin^2\theta\,\mathrm{d}\theta \\
&\times \sum_{l=-\infty}^{+\infty} J_l(qV_E\,\alpha\sin\theta) \\
&\times \Big[J_{l+1}(qV_E\,\beta\sin\theta)\exp\big[\mathrm{i}(2l+1)(\omega t - kz)\big] \\
&+ J_{l-1}(qV_E\,\beta\sin\theta)\exp\big[\mathrm{i}(2l-1)(\omega t - kz)\big]\Big]\,, \qquad \text{(A.1)}
\end{aligned}$$

where

$$\alpha = \frac{e_x + e_y}{2}\,, \qquad \beta = \frac{e_x - e_y}{2}\,.$$

Further, the relationship

$$\begin{aligned}
&\sum_{l=-\infty}^{+\infty} \exp\big[\mathrm{i}(2l+1)(\omega t - kz)\big] \\
&\quad\times \big[J_l(A)\,J_{l+1}(B) + J_{l+1}(A)\,J_l(B)\big] \\
&\quad= 2\mathrm{i}\sum_{l=0}^{\infty}\sin\big[(2l+1)(\omega t - kz)\big] \\
&\quad\times \left[\frac{l}{B} + \frac{l}{A} - \frac{\mathrm{d}}{\mathrm{d}B} - \frac{\mathrm{d}}{\mathrm{d}A}\right] J_l(A)\,J_l(B)\,,
\end{aligned}$$

can be used to write down Eqn (A.1) in the form

$$\begin{aligned}
I_x &= \frac{2\pi\mathrm{i}}{V_E^2}\sum_{l=0}^{\infty}\sin\big[(2l+1)(\omega t - kz)\big]\left[\frac{l}{\alpha} + \frac{l}{\beta} - \frac{\mathrm{d}}{\mathrm{d}\alpha} - \frac{\mathrm{d}}{\mathrm{d}\beta}\right] \\
&\times \int_0^\infty \mathrm{d}x\,x^2\int_0^\pi \mathrm{d}\theta\,\exp\left(-\frac{x^2 V_T^2}{2V_E^2\sin^2\theta}\right) J_l(\alpha x)\,J_l(\beta x)\,. \qquad \text{(A.2)}
\end{aligned}$$

In view of the identity [22]

$$\int_0^{\pi/2}\mathrm{d}\theta\,\exp\left(-\frac{x^2 V_T^2}{2V_E^2\sin^2\theta}\right) = \pi\left[1 - \Phi\left(\frac{xV_T}{\sqrt{2}V_E}\right)\right],$$

where

$$\Phi(z) = \frac{2}{\sqrt{\pi}}\int_0^z \mathrm{d}t\,\exp(-t^2)$$

is the probability integral, we can represent Eqn (A.2) as

$$\begin{aligned}
I_x &= \frac{4\mathrm{i}\pi^{3/2}}{V_E^2}\sum_{l=0}^{\infty}\sin\big[(2l+1)(\omega t - kz)\big]\left[\frac{l}{\alpha} + \frac{l}{\beta} - \frac{\mathrm{d}}{\mathrm{d}\alpha} - \frac{\mathrm{d}}{\mathrm{d}\beta}\right] \\
&\times \int_{V_T/\sqrt{2}V_E}^{\infty}\mathrm{d}\tau\int_0^\infty \mathrm{d}x\,x\exp(-x^2\tau^2)\,J_l(x\alpha)\,J_l(\beta x)\,. \qquad \text{(A.3)}
\end{aligned}$$

We note that [10]

$$\begin{aligned}
&\int_0^\infty \mathrm{d}x\,x\exp(-x^2\tau^2)J_l(\alpha x)\,J_l(\beta x) \\
&\quad= \frac{1}{2\tau^2}\exp\left(-\frac{\alpha^2+\beta^2}{4\tau^2}\right) I_l\left(\frac{\alpha\beta}{2\tau^2}\right),
\end{aligned}$$

where $I_p(x)$ is the Bessel function of the second kind, and substitute the last expression into Eqn (A.2) to obtain, by means of simple rearrangements, the following relationship

$$\begin{aligned}
I_x &= e_x\,\frac{4\sqrt{2}\,\mathrm{i}\pi^2}{V_E^2}\sum_{l=0}^{\infty}\sin\big[(2l+1)(\omega t - kz)\big] \\
&\times \left[A_l\left(\rho^2, \frac{V_E}{2V_T}\right) - A_{l+1}\left(\rho^2, \frac{V_E}{2V_T}\right)\right]. \qquad \text{(A.4)}
\end{aligned}$$

Here, we employed the notation

$$A_l(\rho^2, x) = \frac{2}{\sqrt{\pi}}\int_0^{x^2}\mathrm{d}t\,\sqrt{t}\,\exp(-t)\big[I_l(\rho^2 t) - I_{l+1}(\rho^2 t)\big]\,. \qquad \text{(A.5)}$$

Formulas (A.4), (A.5), and (21) can be utilized to write down the x projection of the right-hand side of Eqn (18) [see formula (24)].

We now carry out a relevant treatment of the y component of the right-hand side of Eqn (19). To this end, we consider

$$I_y = \int \mathrm{d}\mathbf{q}\,\frac{q_y}{q^2}\exp\left(-\mathrm{i}\mathbf{qu} - \frac{1}{2}\,q^2 V_T^2\right)$$
$$= \int_0^{\infty}\mathrm{d}q\,q\exp\left(-\frac{1}{2}\,q^2 V_T^2\right)\int_0^{\pi}\sin^2\theta\,\mathrm{d}\theta\int_0^{2\pi}\mathrm{d}\varphi\sin\varphi$$
$$\times\sum_{l=-\infty}^{+\infty}\sum_{n=-\infty}^{+\infty}J_l(qV_E\alpha\sin\theta)\,J_n(qV_E\beta\sin\theta)$$
$$\times\exp\left[\mathrm{i}(l+n)(\omega t - kz)\right]\exp\left[\mathrm{i}(l-n)\varphi\right]$$
$$= -\frac{\mathrm{i}\pi}{V_E^2}\int_0^{\infty}\mathrm{d}x\int_0^{\pi}\mathrm{d}\theta\,\exp\left(-\frac{V_T^2x^2}{2V_E^2\sin^2\theta}\right)$$
$$\times\sum_{l=-\infty}^{+\infty}\exp\left[\mathrm{i}(2l+1)(\omega t - kz)\right]$$
$$\times\left[J_l(x\alpha)\,J_{l+1}(x\beta) - J_{l+1}(\alpha x)\,J_l(\beta x)\right]. \qquad (A.6)$$

Next, we use the relationship

$$\sum_{l=-\infty}^{+\infty}\exp\left[\mathrm{i}(2l+1)(\omega t - kz)\right]$$
$$\times\left[J_l(A)\,J_{l+1}(B) - J_{l+1}(A)\,J_l(B)\right]$$
$$= 2\sum_{l=0}^{\infty}\cos\left[(2l+1)(\omega t - kz)\right]$$
$$\times\left[\frac{l}{B} - \frac{l}{A} + \frac{\mathrm{d}}{\mathrm{d}A} - \frac{\mathrm{d}}{\mathrm{d}B}\right]J_l(A)\,J_l(B)\,,$$

with a parallel recast of the integral with respect to θ in Eqn (A.6), yielding the representation

$$I_y = -\frac{4\mathrm{i}\pi^{3/2}}{V_E^2}\sum_{l=0}^{\infty}\cos\left[(2l+1)(\omega t - kz)\right]$$
$$\times\left[\frac{l}{\beta} - \frac{l}{\alpha} + \frac{\mathrm{d}}{\mathrm{d}\alpha} - \frac{\mathrm{d}}{\mathrm{d}\beta}\right]$$
$$\times\int_{V_T/\sqrt{2}V_E}^{\infty}\mathrm{d}\tau\int_0^{\infty}\mathrm{d}x\,x\exp\left(-x^2\tau^2\right)J_l(x\alpha)\,J_l(\beta x)\,. \qquad (A.7)$$

Since this expression is largely analogous to Eqn (A.3), we can carry out rearrangements similar to that done in considering Eqn (A.3), thus arriving at

$$I_y = e_y\,\frac{4\sqrt{2}\,\mathrm{i}\pi^2}{V_E^2}\sum_{l=0}^{\infty}\cos\left[(2l+1)(\omega t - kz)\right]$$
$$\times\left[A_l\left(\rho^2, \frac{V_E}{2V_T}\right) + A_{l+1}\left(\rho^2, \frac{V_E}{2V_T}\right)\right]. \qquad (A.8)$$

According to Eqn (21), this relationship makes it possible to obtain expression (25).

References

1. Artsimovich L A *Upravlyaemye Termoyadernye Reaktsii* (Controlled Thermonuclear Reactions) (Moscow: Fizmatgiz, 1961) [Translated into English (New York: Gordon and Breach, 1964)]
2. Silin V P *Zh. Eksp. Teor. Fiz.* **47** 2254 (1964) [*Sov. Phys. JETP* **20** 1510 (1965)]
3. Gladkov S M, Koroteev N I *Usp. Fiz. Nauk* **160** (7) 105 (1990) [*Sov. Phys. Usp.* **33** 554 (1990)]
4. Svanberg S et al. *Phys. Scripta* **49** 187 (1994)
5. Krause J L, Schafer K J, Kulander K C *Phys. Rev. Lett.* **68** 3535 (1992)
6. Wahlström C-G et al. *Phys. Rev. A* **48** 4709 (1993)
7. Kondo K et al. *Phys. Rev. A* **49** 3881 (1994)
8. Preston S G et al. *Phys. Rev. A* **53** R31 (1996)
9. Giammanco F et al. *Laser Phys.* **7** 22 (1996)
10. Schulz H, von der Linde D *Proc. SPIE* **1268** 30 (1990)
11. Silin V P *Zh. Eksp. Teor. Fiz.* **114** 864 (1998) [*JETP* **87** 468 (1998)]
12. Ovchinnikov K N, Silin V P *Kvantovaya Elektron.* **29** (11) 145 (1999) [*Quantum Electron.* **29** 983 (1999)]
13. Fedotov A B et al. *Phys. Lett. A* **271** 407 (2000)
14. Silin V P *Zh. Eksp. Teor. Fiz.* **117** 926 (2000) [*JETP* **90** 805 (2000)]
15. Silin V P *Phys. Lett. A* **286** 190 (2001)
16. Burnett N H, Kan C, Corkum P B *Phys. Rev. A* **51** R3418 (1995)
17. Landau L D, Lifshitz E M *Teoriya Polya* (The Classical Theory of Fields) (Moscow: Nauka, 1973) [Translated into English (Oxford: Pergamon Press, 1975)]
18. Silin V P, Silin P V *Fiz. Plazmy* **32** 755 (2006) [*Plasma Phys. Rep.* **32** 695 (2006)]
19. Silin V P, Silin P V *Fiz. Plazmy* **33** (2) (2007) [*Plasma Phys. Rep.* **33** 153 (2007)]
20. Silin V P, Silin P V, in *ECLIM 2002: 27th Eur. Conf. on Laser Interaction with Matter* (Proc. SPIE, Vol. 5228, Eds O N Krokhin, S Yu Gus'kov, Yu A Merkul'ev) (Bellingham, Wash.: SPIE, 2003)
21. Haberland H, Bonitz M, Kremp D *Phys. Rev. E* **64** 026405 (2001)
22. Gradshteyn I S, Ryzhik I M *Tablitsy Integralov, Summ, Ryadov i Proizvedenii* (Tables of Integrals, Sums, Series, and Products) 4th ed. (Moscow: Fizmatgiz, 1962) [Translated into English (New York: Academic Press, 1965)]
23. Fock V *Z. Phys.* **98** 145 (1935)
24. Vagin K Yu, Ovchinnikov K N, Silin V P *Kvantovaya Elektron.* **34** 223 (2004) [*Quantum Electron.* **34** 223 (2004)]
25. Silin V P, Silin P V *Kvantovaya Elektron.* **35** 531 (2005) [*Quantum Electron.* **35** 531 (2005)]
26. Silin V P, Silin P V *Ukrainian J. Phys.* **50** (8A) A10 (2005)
27. Lebedev V S, Beigman I L *Physics of Highly Excited Atoms and Ions* (Springer Ser. on Atoms + Plasmas, Vol. 22) (Berlin: Springer-Verlag, 1998)
28. Silin V P, Silin P V *Kvantovaya Elektron.* **33** 897 (2003) [*Quantum Electron.* **33** 897 (2003)]